

Compositional tuning of atomic layer deposited MgZnO for thin film transistors

J. S. Wrench, I. F. Brunell, P. R. Chalker, J. D. Jin, A. Shaw, I. Z. Mitrovic, and S. Hall

Citation: *Appl. Phys. Lett.* **105**, 202109 (2014); doi: 10.1063/1.4902389

View online: <https://doi.org/10.1063/1.4902389>

View Table of Contents: <http://aip.scitation.org/toc/apl/105/20>

Published by the [American Institute of Physics](#)

Articles you may be interested in

[A comprehensive review of ZnO materials and devices](#)

Journal of Applied Physics **98**, 041301 (2005); 10.1063/1.1992666

[Atomic layer deposition of Nb-doped ZnO for thin film transistors](#)

Applied Physics Letters **109**, 222103 (2016); 10.1063/1.4968194

[Metal oxide semiconductor thin-film transistors for flexible electronics](#)

Applied Physics Reviews **3**, 021303 (2016); 10.1063/1.4953034

[Wide-bandgap high-mobility ZnO thin-film transistors produced at room temperature](#)

Applied Physics Letters **85**, 2541 (2004); 10.1063/1.1790587

[ZnO-based transparent thin-film transistors](#)

Applied Physics Letters **82**, 733 (2003); 10.1063/1.1542677

[Transparent ZnO thin-film transistor fabricated by rf magnetron sputtering](#)

Applied Physics Letters **82**, 1117 (2003); 10.1063/1.1553997

AIP | Conference Proceedings

Get **30% off** all
print proceedings!

Enter Promotion Code **PDF30** at checkout



Compositional tuning of atomic layer deposited MgZnO for thin film transistors

J. S. Wrench,¹ I. F. Brunell,¹ P. R. Chalker,¹ J. D. Jin,² A. Shaw,² I. Z. Mitrovic,² and S. Hall²

¹Centre for Materials and Structures, School of Engineering, University of Liverpool, Ashton Street, Liverpool L69 3GH, United Kingdom

²Department of Electrical Engineering and Electronics, University of Liverpool, Brownlow Hill, Liverpool L69 3GJ, United Kingdom

(Received 10 September 2014; accepted 11 November 2014; published online 20 November 2014)

Thin film transistors (TFTs) have been fabricated using magnesium zinc oxide (MgZnO) layers deposited by atomic layer deposition at 200 °C. The composition of the MgZnO is systematically modified by varying the ratio of MgO and ZnO deposition cycles. A blue-shift of the near band-edge photoluminescence after post-deposition annealing at 300 °C indicates significant activation of the Mg dopant. A 7:1 ratio of ZnO:MgO deposition cycles was used to fabricate a device with a TFT channel width of 2000 μm and a channel length of 60 μm. This transistor yielded an effective saturation mobility of 4 cm²/V s and a threshold voltage of 7.1 V, respectively. The on/off ratio was 1.6 × 10⁶ and the maximum interface state density at the ZnO/SiO₂ interface is ~6.5 × 10¹² cm⁻². © 2014 AIP Publishing LLC. [<http://dx.doi.org/10.1063/1.4902389>]

Zinc oxide (ZnO)-based thin film transistors (TFTs) are attractive candidates for transparent electronics. Conventional TFT materials, such as hydrogenated amorphous silicon (a-Si:H), benefit from ambient deposition conditions and ease of processing. However, such devices exhibit relatively small mobility ($\mu_{\text{eff}} < 1 \text{ cm}^2/\text{V s}$),¹ which is too low for high-speed switching in flat panel displays, especially for 3D and high-resolution large-area displays which require high refresh rates. As an alternative, RF-sputtered magnesium zinc oxide (MgZnO) has been explored as a TFT material.² The benefits of adding Mg to ZnO are cited as a larger band gap (7.7 eV for MgO and 3.28 eV for ZnO) and lower oxygen-related defect concentrations because of the higher oxygen-affinity of magnesium. This view is substantiated by Ku *et al.*,³ who have used metal-organic chemical vapour deposition to deposit Mg_{0.06}Zn_{0.94}O as an active layer in TFTs with superior thermal stability compared to pure ZnO devices. In this paper, we use atomic layer deposition (ALD) to deposit MgZnO channels in TFTs. ALD has become a mainstream process for the manufacture of high-κ dielectrics in silicon electronic devices and elsewhere. For example, ALD has been used to deposit Mg_xZn_{1-x}O films which have been investigated for use as buffer layers in Cu(In,Ga)Se₂-based solar cells.⁴ The Mg_xZn_{1-x}O films were grown using diethyl zinc (DEZn), bis(cyclopentadienyl) magnesium (MgCp₂), and water as precursors in the temperature range from 105 to 180 °C. Single-phase ZnO-like films were obtained for $x < 0.2$, followed by a two-phase region of ZnO- and MgO-like structures for higher Mg concentrations. Increasing optical band gaps of up to above 3.8 eV was obtained for Mg_xZn_{1-x}O with increasing x . In this paper, we report the use of ALD to fabricate a range of Mg_xZn_{1-x}O thin film transistors and the influence that composition has on the material and device characteristics.

The atomic layer deposition experiments were performed using the liquid DEZn and bis(ethylcyclopentadienyl)magnesium, Mg(CpEt)₂ sources, which were delivered, at room temperature and 95 °C, respectively, into the process

chamber from independent sources. Mg_xZn_{1-x}O films are deposited using x cycles of ZnO steps via exposure of the surface to successive steps of DEZn and then water vapour. Intermittent pump purge steps are used to prevent gas-phase pre-reaction, which ensures the surface reaction. After the x ZnO cycles, a single MgO cycle is deposited via exposure of the surface to successive steps of Mg(CpEt)₂ and then water vapour. The whole process is repeated N times until the desired film thickness has been achieved. For example, a film using a ZnO:Mg ratio of 9:1 where $x = 9$ and $N = 30$ gives a total number of 270 DEZn and 30 Mg(CpEt)₂ ALD cycles. This equates to a Mg(CpEt)₂ cycle fraction of 0.1 (1/(9 + 1)). A range of films using the cycle ratios of ZnO:Mg of 2:1, 3:1, 5:1, 7:1, 8:1, 9:1, 10:1, 20:1, and 49:1 were tested. Crystallographic characterisation of the Mg_xZn_{1-x}O films was performed using X-ray diffraction (XRD) and room temperature photoluminescence (PL) spectroscopy. The films were deposited on soda lime glass substrates at 200 °C and were subsequently annealed at 300 °C in air for 1 h. The crystalline phases were identified by XRD using Cu Kα radiation (0.154051 nm, 40 kV, and 50 mA) and diffraction patterns from a sample of the annealed films are shown in Fig. 1(a). The crystalline texture of the films undergoes some significant changes across the composition range studied. As the Mg incorporation increases from 49:1 to 7:1, the c -axis (002) oriented growth diminishes, which is indicated by the decreasing ratio of the (002) diffraction peak with respect to the (100) and (101) peaks. Notably, the full-width at half maxima (FWHM) of the diffraction peaks remains unchanged, suggesting that the crystalline domain size is fairly constant. PL data were excited using 325 nm (3.82 eV) excitation from a He-Cd laser. Spectra were acquired using a Raman confocal microscope set to 100 μm aperture coupled to a single grating spectrometer equipped with a notch filter and a CCD camera detector. The PL spectra acquired from a 7:1 Mg_xZn_{1-x}O film deposited at 200 °C on glass are shown in Fig. 1(b). The as-deposited film exhibits a peak emission at 3.38 eV and is attributed to near

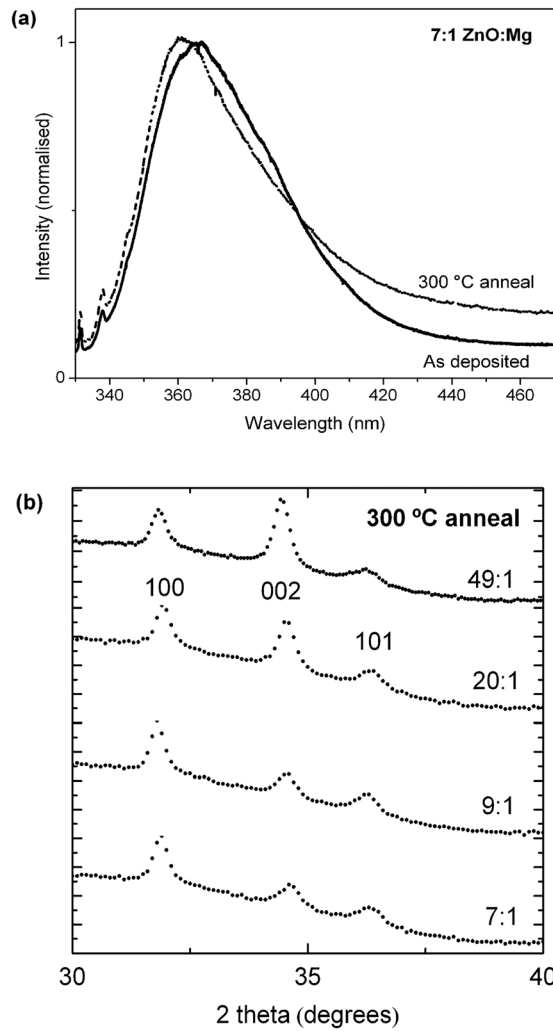


FIG. 1. (a) UV photoluminescence of as deposited (solid line) and 300 °C annealed (dashed) 7:1 ZnO:Mg films and (b) X-ray diffraction patterns of ZnO:Mg films deposited using varying cycle ratios.

band-edge emission arising from the recombination of free excitons. The film was subsequently annealed at 300 °C in air for 1 h and the PL spectrum from this film was observed to blue-shift to 3.44 eV. The band gap of $Mg_xZn_{1-x}O$ alloys is known to increase with [Mg] content via the Burstein-Moss effect,^{5,6} in which magnesium-induced charge carriers occupy states just above the bottom of the ZnO conduction band. This has the effect of pushing the absorption edge to higher energies. The same effect has been observed in gallium-doped ZnO deposited by ALD.⁷ In the present case, the blue-shift effect is ascribed to the increased activation of the Mg dopant from the deposition temperature at 200 °C to the higher 300 °C annealing.

$Mg_xZn_{1-x}O$ films were grown at 200 °C via the ALD technique on a highly doped *n*-type silicon wafer with a 50 nm thermally oxidised SiO_2 layer, which served as a gate dielectric for the TFT. The Mg doped films were grown to a thickness of 50 nm where the cycle ratio between the ZnO and Mg precursors ranged from 10:1 to 2:1. Source/drain electrodes with a thickness of 100 nm were fabricated by evaporating aluminium through a shadow mask, which defined a TFT channel width (W) of 2000 μm and a channel length (L) of 60 μm . Finally, the devices were subjected to

the same thermal annealing process used for the samples above. A schematic of the fabricated bottom-gated ZnO TFTs is shown in the inset of Fig. 2(b). The electrical characteristics of ZnO TFTs were measured at room temperature in the dark using an Agilent B1500 semiconductor parameter analyser. Fig. 2 shows a range of characteristics for MgZnO TFTs as a function of the fraction of Mg ALD doping cycles. Figs. 2(a) and 2(b) show an effective field effect mobility in the saturation region and threshold voltage which were extracted using the standard equation for source-drain saturation current

$$I_{DS} = \frac{C_i \mu_{SAT} W}{2L} (V_{GS} - V_T)^2 \text{ for } V_{DS} > V_{GS} - V_T, \quad (1)$$

where C_i is the gate capacitance per unit area, μ_{SAT} is the mobility in the saturation region, V_{GS} is the gate voltage referenced to the source, and V_T is the threshold voltage. It is recognised that ZnO TFTs tend to follow a power law dependence⁸ but the form of Eq. (1) is used conventionally for purposes of comparison. The effective mobility in the saturation region shows a tendency to decrease from 4.32 to 0.47 $cm^2/V \cdot s$ as the magnesium cycle fractions increase across range from 0.09 (10:1 ZnO:Mg) to 0.33 (2:1). The FWHM of the X-ray diffraction data for these films indicates an approximately constant grain size, which suggests that impurity scattering rather than grain boundary scattering has some influence in these thin channel materials, although the effect of a reported increased electron effective mass due to band-gap widening may not be neglected.⁹ The threshold

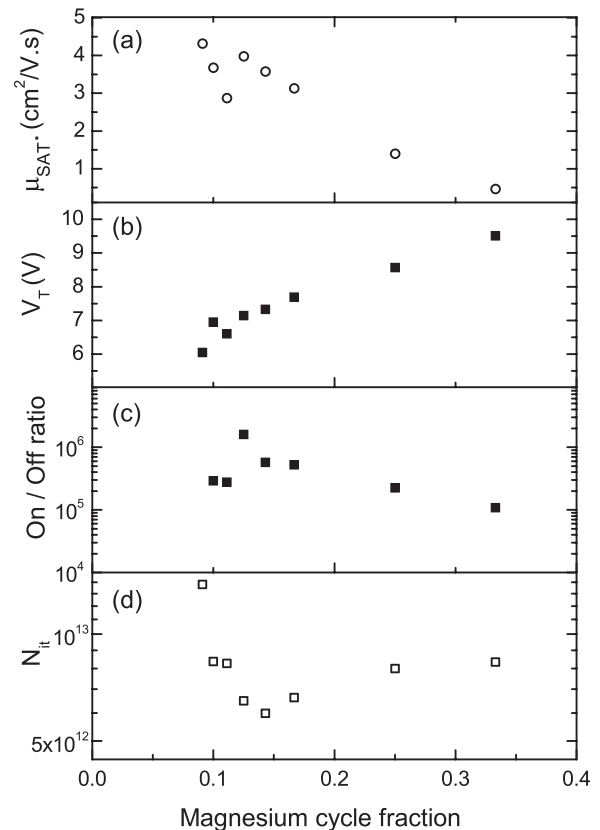


FIG. 2. Characteristics of TFTs with varying Mg doping cycle fractions. (a) Saturation field-effect mobility, (b) threshold voltage, (c) on/off ratio, and (d) interface trap density.

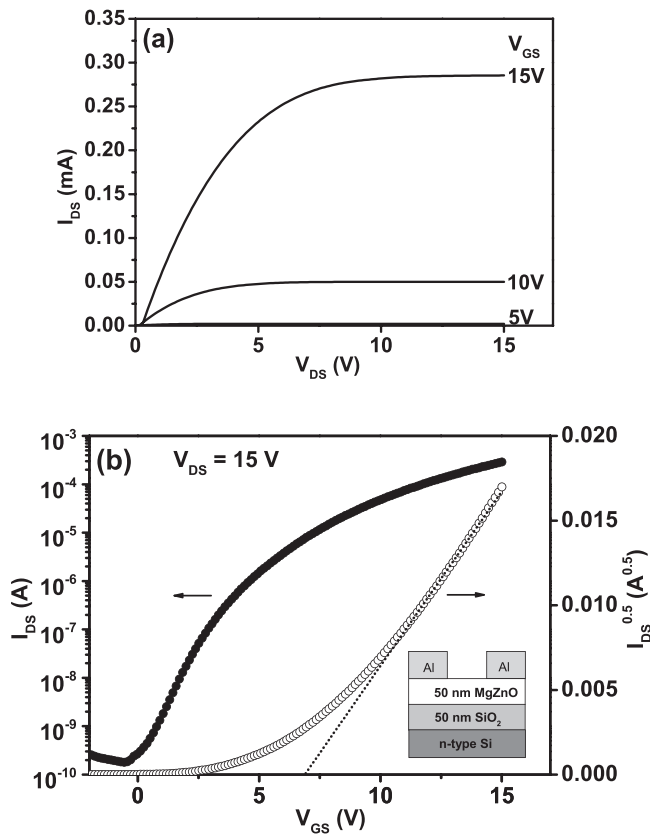


FIG. 3. (a) Output and (b) transfer characteristics of a 7:1 ALD Mg doped ZnO TFT. Square root of drain current and a linear fit (dashed line) are also shown in (b). The inset shows a schematic of the ZnO TFTs.

voltage for the devices exhibits the opposite trend increasing from 6.05 V to 9.51 V, respectively. The variation of on/off ratio with magnesium content shown in Fig. 2(c) exhibits a maximum at a doping cycle fraction of 0.13 (7:1). From the transfer characteristics, an effective sub-threshold swing (S) can be extracted using the equation

$$S = \frac{dV_{GS}}{d(\log I_{DS})}, \quad (2)$$

where S can be obtained from the experimental characteristics assuming an exponential dependence of the current at low voltage. From S , the maximum density of surface state (N_{it}) at the channel/dielectric interface can be estimated using the following equation:¹⁰

$$N_{it} = \left[\frac{S \log(e)}{(kT/q)} - 1 \right] \frac{C_i}{q}, \quad (3)$$

where k is Boltzmann's constant, e is the base of the natural logarithm, T is the absolute temperature, and q is the electron charge. The variation in the interface state density (N_{it}) at the MgZnO/SiO₂ interface for the doping range investigated is shown in Fig. 2(d) and a minimum was observed for the 7:1 composition. This observation is contrary to the interface state densities reported for RF co-sputtered MgZnO TFTs deposited onto SiO₂/n⁺-Si substrates at 300 °C.¹¹ In that study, it was found that the addition of magnesium generally

increased N_{it} . This can be explained by the ALD doping mechanism in which the doped ZnO interface with the underlying SiO₂ is predominantly ZnO-like. From the parameters presented in Fig. 2, it is apparent that the optimum TFT performance, in terms of on/off ratio, was achieved for the ZnO:Mg 7:1 composition. Fig. 3 shows (a) the output and (b) the transfer characteristics for a typical MgZnO TFT fabricated using the 7:1 process. This TFT operates as an n -channel, accumulation-mode device, where there is good saturation at high drain bias. The effective mobility in the saturation region and the effective threshold voltage (defined as the gate-source voltage derived from Eq. (1)) obtained for the device were 4 cm²/V s and 7.1 V, respectively. The on/off current ratio was observed to be 1.6×10^6 and the maximum effective interface state density at the ZnO/SiO₂ interface is $\sim 6.5 \times 10^{12}$ cm⁻².

Atomic layer deposition has been used to grow films of Mg_xZn_{1-x}O for use as a TFT channel with varying Mg content controlled by changing the cycle ratios to investigate mobility, on/off ratio, and interface density of states. Optimum TFT performance was achieved with a ZnO:Mg composition of 7:1. The TFT characteristics are comparable to similar grown ALD ZnO devices^{12,13} and demonstrate that atomic layer deposition represents a viable alternative for sputtering techniques.² In addition, ALD process technology has inherent advantages in terms of batch processing and scaling compared with other thin film procedures.¹⁴ This study shows the potential for exploiting MgZnO alloys in ZnO-based display technologies.

The authors would like to thank the Engineering and Physical Sciences Research Council for funding to carry out this research (Project No. EP/K018884/1).

¹Y. Kuo, IEEE Proceedings of 2013 Twentieth international workshop on activematrix flat panel displays and devices (AM-FPD 13): TFT technologies and FPD materials, pp. 5–8 (2013).

²Y.-S. Tsai and J.-Z. Chen, *IEEE Trans. Electron Devices* **59**, 151 (2012).

³C.-J. Ku, Z. Duan, P. I. Reyes, Y. Lu, Y. Xu, C.-L. Hsueh, and E. Garfunkel, *Appl. Phys. Lett.* **98**, 123511 (2011).

⁴T. Törndahl, C. Platzer-Björkman, J. Kessler, and M. Edoff, *Prog. Photovoltaics* **15**, 225 (2007).

⁵C. Y. Liu, H. Y. Xu, L. Wang, X. H. Li, and Y. C. Liu, *J. Appl. Phys.* **106**, 073518 (2009).

⁶L. Gao and J.-M. Zhang, *Acta Phys. Sin.* **59**, 1263 (2010).

⁷A. Segura, J. A. Sans, D. Errandonea, D. Martínez-García, and V. Fages, *Appl. Phys. Lett.* **88**, 011910 (2006).

⁸F. Torricelli, J. R. Meijboom, E. Smits, A. K. Tripathi, M. Ferroni, S. Federici, G. H. Gelinck, L. Colalongo, Z. M. Kovacs-Vajna, D. De Leeuw, and E. Cantatore, *IEEE Trans. Electron Devices* **58**, 2610 (2011).

⁹A. A. Ziabari and S. M. Rozati, *Physica B* **407**, 4512 (2012).

¹⁰J. K. Jeong, J. H. Jeong, H. W. Yang, J. S. Park, Y. G. Mo, and H. D. Kim, *Appl. Phys. Lett.* **91**, 113505 (2007).

¹¹J. H. Lee, C. H. Kim, H. S. Kim, N. W. Jang, Y. Yun, L. M. Do, and K. H. Baek, *J. Korean Phys. Soc.* **62**, 937 (2013).

¹²S. Kwon, S. Bang, S. Lee, S. Jeon, W. Jeong, H. Kim, S. C. Gong, H. J. Chang, H.-h. Park, and H. Jeon, *Semicond. Sci. Technol.* **24**, 035015 (2009).

¹³J. Yang, J. K. Park, S. Kim, W. Choi, S. Lee, and H. Kim, *Phys. Status Solidi A* **209**, 2087 (2012).

¹⁴H. B. Profijt, S. E. Potts, M. C. M. Van de Sanden, and W. M. M. Kessels, *J. Vac. Sci. Technol., A* **29**, 050801 (2011).